

Red and Blue Liquid-Crystalline Borondipyrromethene Dendrimers

Soumyaditya Mula,^{†,‡} Stéphane Frein,[#] Virginie Russo,[#] Gilles Ulrich,[†] Raymond Ziessel,^{*,†} Joaquín Barberá,^{*,§} and Robert Deschenaux^{*,#}

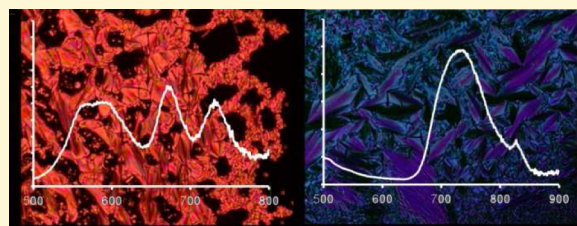
[†]ICPEES-LCOSA, CNRS, UMR 7515, Ecole de Chimie, Polymères, Matériaux de Strasbourg (ECPM), 25 rue Becquerel, 67087 Strasbourg, Cedex 02, France

[§]Departamento de Química Orgánica, Facultad de Ciencias-Instituto de Ciencia de Materiales de Aragón, Universidad de Zaragoza-CSIC, 50009 Zaragoza, Spain

[#]Institut de Chimie, Université de Neuchâtel, Avenue de Bellevaux 51, 2000 Neuchâtel, Switzerland

Supporting Information

ABSTRACT: We have designed a series of modular and fluorescent poly(arylester) dendrimers functionalized with cyanobiphenyl subunits and fluorescent borondipyrromethene (Bodipy) dyes. The green emitter is a Bodipy with four methyl groups, and the Bodipy dye possessing extended conjugation with two methyl and two vinyl groups acts as a red emitter. The design element of these architectures relates to a secondary amide linkers interposed between the conventional Bodipy and the dendrons. The second- and third-generation dendrimers give rise to nematic and/or smectic A phases, whereas the first-generation dendrimers show smectic A and C phases or an unidentified mesophase. The novel materials are highly fluorescent in solution and in the as-obtained powders but not in the mesophase. Dilution of the dendritic dyes with the nonfluorescent acid dendron in the solid phase shifted the fluorescence to higher energy, and demonstrated the presence of aggregates in the solid state. Mixing the red and blue materials in a solid phase led to the observation of effective electronic energy transfer from the red dye to the blue one. Increasing the proportion of the red dye (energy donor) from 1 to 250 molar with respect to the blue dye (energy acceptor) resulted in the observation of residual emission of the red dye in the solid state mixture. Increasing the proportion from 1 to 1000 resulted in equal emission in the 540 to 760 nm range.



INTRODUCTION

Much attention is devoted to the design of amphiphilic dendrimers because of their potential applications in nanosciences¹ and biomedicine.^{2,3} Contrary to conventional liquid-crystalline (LC) materials, dendritic platforms tolerate various functional groups whose shape, molecular volume, and physical properties can be counterbalanced by the size (generation) of the dendrimers as well as by the nature of the functional groups required to favor microsegregation within the mesophases.⁴ Several modular and self-assembled systems have been reported, including liquid-crystalline [60]fullerenes,⁵ ferrocenes,⁶ [60]-fullerene-ferrocene dyads,⁷ diruthenium clusters,⁸ flat fluorescent dyes,⁹ and gold nanoparticles.¹⁰ Recently, libraries of amphiphilic dendrimers carrying monosaccharides (D-mannose and D-galactose) and disaccharides (D-lactose) in their hydrophilic parts, have been engineered, and their ligand bioactivity demonstrated.³

Luminescent liquid-crystalline materials have recently gained much importance because of their novel and specific utilizations, such as (i) to tune the mesophase arrangements by photoisomerization of specific items (e.g., azo or vinyl functions), (ii) to favor charge mobility and charge separation along columnar organization, and (iii) to promote sensing properties in the gel phase or mesophases.^{11–14} The introduction of packing changes in a luminescent self-assembled condensed phase through the

use of external stimuli (e.g., photon¹⁵ or mechanical stress^{11,16}) might find interesting applications in optoelectronic devices and sensors. Recently, photoresponsible self-assembly of vesicles prone by a host–guest azobenzene/ β -cyclodextrin interaction, and dismantled by the trans/cis azo isomerization under photonic stimulation, has been studied.¹⁷ Phosphorescent liquid-crystalline platinum and iridium complexes^{18,19} have also been studied and show the importance of the geometry and space filling of the chromophore in the packing of the molecules within the mesophases and on the luminescence properties. Thermotropic luminescent palladium(II) ortho-metallated imine²⁰ or N-benzoylthiourea complexes,²¹ and luminescent molybdenum nanoclusters also exhibit interesting liquid-crystalline properties.²²

We have previously shown that borondipyrromethene dyes adequately substituted with a 3,5-diacylamidotoluene platform equipped with two lateral aromatic rings each bearing three appended aliphatic chains give rise to fluorescent organogels²³ and liquid-crystalline materials with columnar organization.²⁴ At that time, the synthetic procedure was known to prepare 4,4'-difluoro-4-bora-3a,4a-diaza-s-indacene (F-Bodipy) derivatives

Received: September 29, 2014

Revised: February 24, 2015

Chart 1

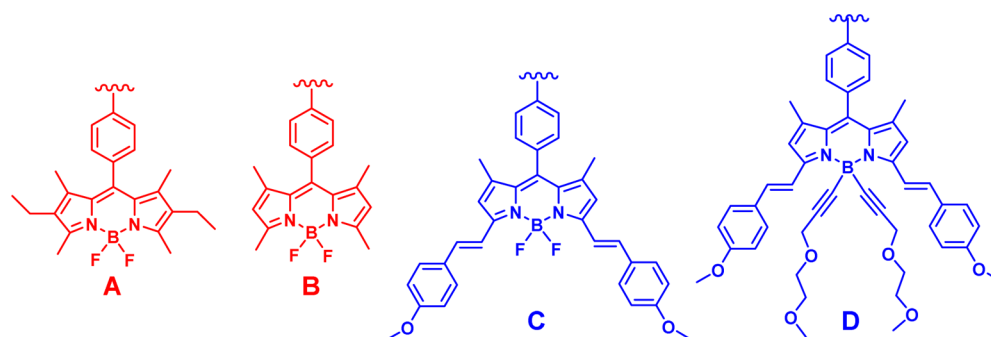
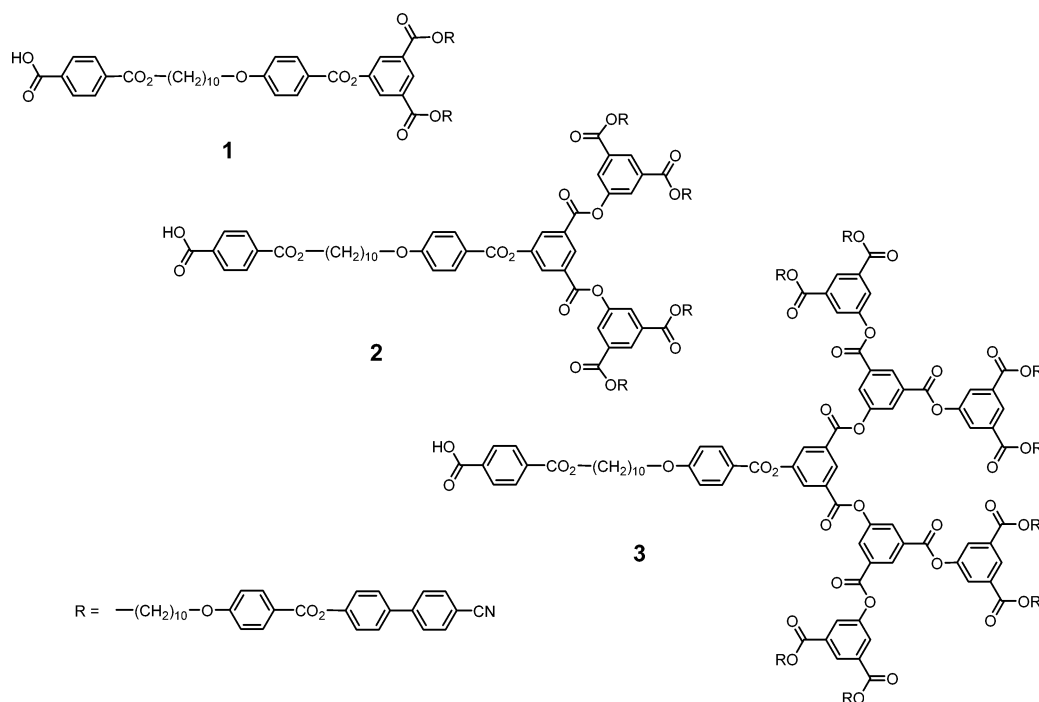
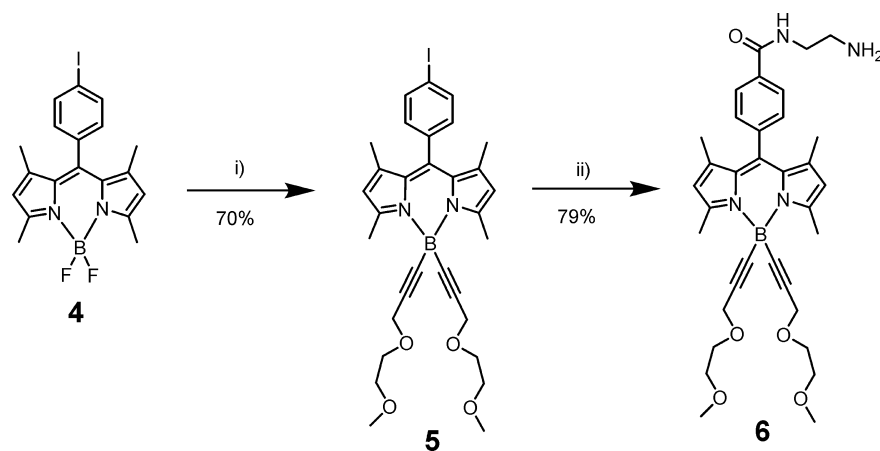
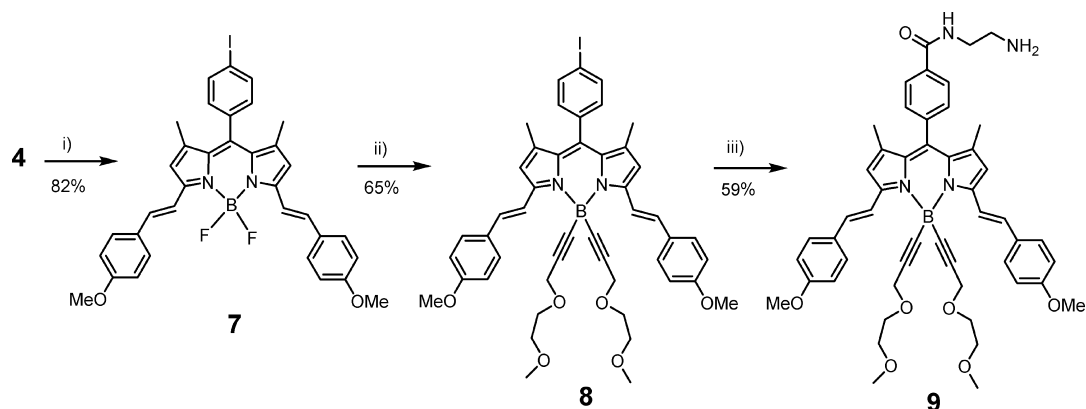


Chart 2

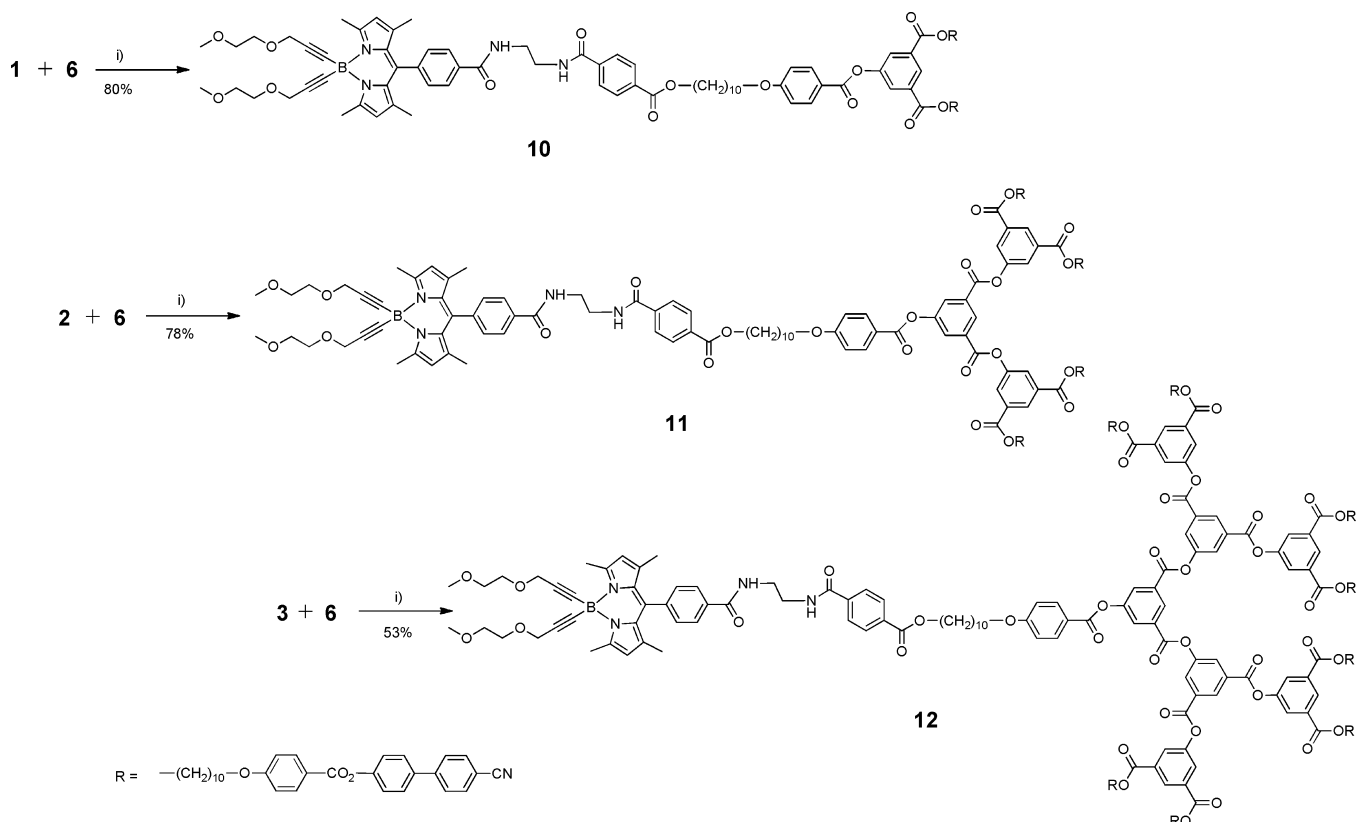
Scheme 1^a

^aReagents and conditions: (i) $\text{CH}_3\text{OCH}_2\text{CH}_2\text{OCH}_2\text{C}\equiv\text{CMgBr}$, dry THF, 60 °C, 12 h; (ii) Et_3N , $\text{H}_2\text{NCH}_2\text{CH}_2\text{NH}_2$, CO, $[\text{Pd}(\text{PPh}_3)_2\text{Cl}_2]$, toluene, 70 °C, 24 h.

(structure A in Chart 1) with red color (λ_{abs} about 520 nm) only. These mesophases display remarkable optoelectronic properties

Scheme 2^a

^aReagents and conditions: (i) *p*-methoxybenzaldehyde, piperidine, toluene, reflux. (ii) $\text{CH}_3\text{OCH}_2\text{CH}_2\text{OCH}_2\text{C}\equiv\text{CMgBr}$, dry THF, 60 °C, 12 h. (iii) Et_3N , $\text{H}_2\text{NCH}_2\text{CH}_2\text{NH}_2$, CO, $[\text{Pd}(\text{PPh}_3)_2\text{Cl}_2]$, toluene, 70 °C, 24 h.

Scheme 3^a

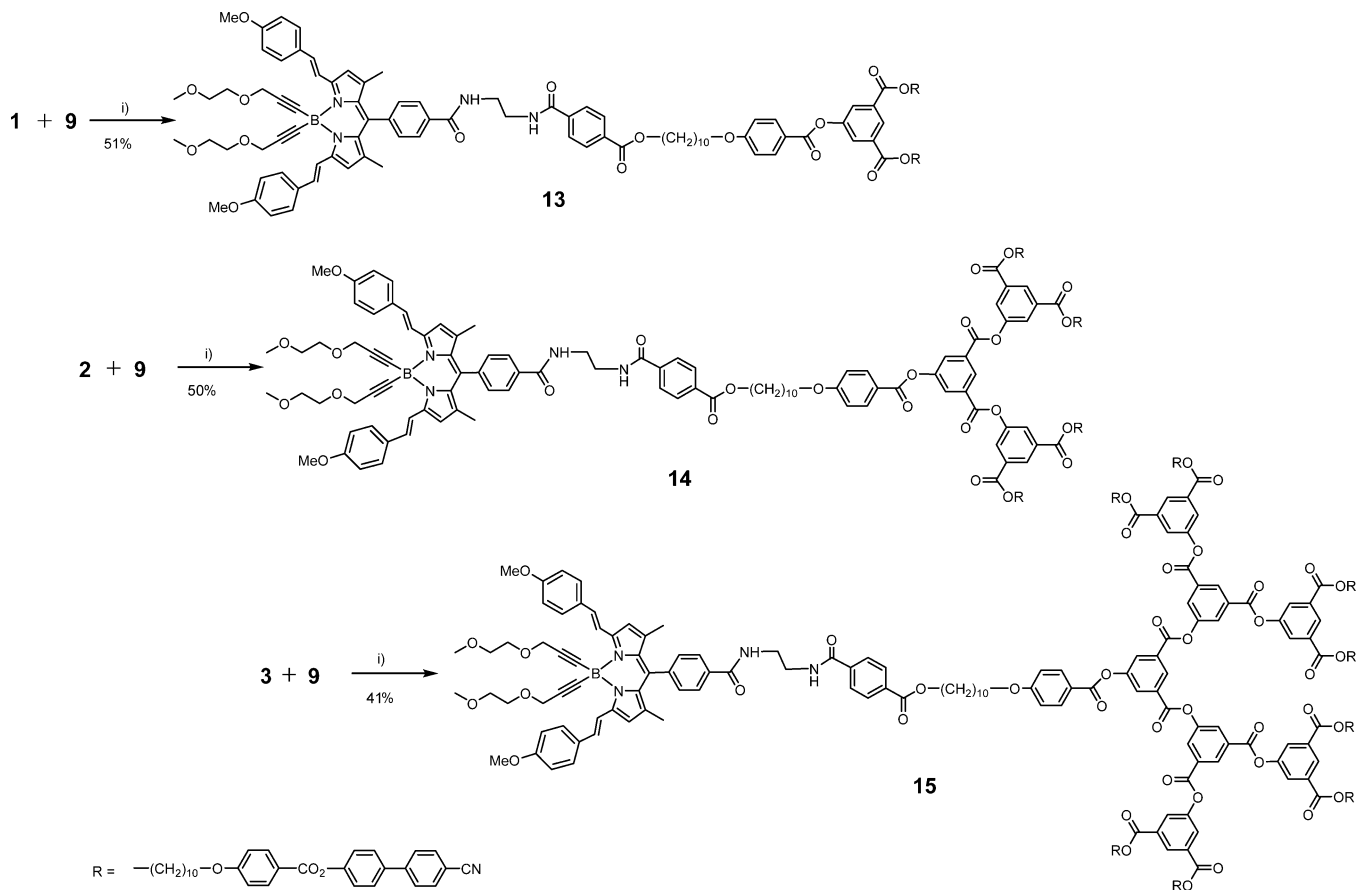
^aReagents and conditions: (i) EDCl, DMAP, CH_2Cl_2 , 48 h.

with strong absorption in the visible region, high fluorescence quantum yields and relatively narrow emission bandwidths with high peak intensities.^{9b,25}

The recent engineering of blue Bodipy dyes (structures C and D in Chart 1) constructed from the red dye B (Chart 1) by an extended divinyl central core opens the doors to the preparation of liquid-crystalline materials with different colors. We have exploited this concept by constructing Bodipy dyes with opposite charges: the blue dye carries an ammonium function while the red dye is made of two sulfonate anions. The ionic-self-assembly of these dyes in a 2:1 blue-to-red stoichiometry affords liquid-crystalline materials with columnar phases in which very efficient

fluorescence energy transfer from the central red dye to the external blue dye occurs in solution and in the columnar phases.²⁵ However, the materials tend to decompose above 200 °C, and the isotropic melt could not be reached.

In this account, we report the successful preparation and characterization of dendritic red and blue liquid-crystalline materials and demonstrate efficient energy transfer from the red to blue dyes in the condensed phase prepared by mixing both materials. However, these materials are not fluorescent in the mesophases.

Scheme 4^a

^aReagents and conditions: (i) EDCI, DMAP, CH_2Cl_2 , 48 h.

RESULTS AND DISCUSSION

Materials and Syntheses. The design is based on first-, second-, and third-generation dendrons bearing a carboxylic acid function (Chart 2)^{9b} and Bodipy dyes having a flexible amino function.²⁶ The use of a tiny linker between the dendron and the dye is required because of the poor nucleophilicity of the *meso*-anilino blue dyes,²⁷ which did not allow coupling with dendrons of different generations. The use of diethylenediamine as a linker allows Schotten–Baumann cross-linking between the dendrons and the dyes under mild reaction conditions after activation of the acid.²⁸

The key Bodipy dyes were prepared as illustrated in Schemes 1 and 2. The red dye **4** was synthesized by the condensation of 2,4-dimethylpyrrole and *p*-iodobenzoyl chloride followed by ring closure with $\text{BF}_3 \cdot \text{Et}_2\text{O}$.²⁹ The blue dye **7** was synthesized via Knoevenagel condensation of **4** and *p*-methoxybenzaldehyde in concentrated solution and at high temperature.³⁰ Substitution of both fluorides of **4** and **7** was feasible using the Grignard reagent of 2,5-dioxaocetyne. The reaction proceeded smoothly and furnished compounds **5** and **8**, respectively. The new peaks at δ 81.1 and 91.5 ppm for the alkyne carbons in the ^{13}C NMR spectrum, and a singlet at δ -10.00 ppm in the ^{11}B NMR spectrum confirmed the formation of **5**. Similar characteristic peaks in the spectrum of **8** were also observed. Then, a Pd catalyzed carboamidation reaction of **5** and **8** in the presence of a flux of CO and an excess of ethylenediamine furnished the red Bodipy **6** and blue Bodipy **9** with primary amine residues which were necessary for the subsequent coupling with the acid

derivatives (Schemes 3 and 4).³¹ The structures were confirmed by spectroscopic methods. For example, the IR peaks at 1644 and 3332 cm^{-1} and the ^{13}C NMR peaks at δ 41.3, δ 42.2, and δ 167.0 ppm confirmed the molecular structure of **6**. It was anticipated that the additional tiny styryl groups in **9** would not change the basic assembly structure of the liquid crystals obtained from the same generation of dendrimer and the red dye **6**.

The dye **6** was coupled with dendrons **1**, **2**, or **3** via peptide coupling reaction using 1-ethyl-3-(3-(dimethylamino)propyl)carbodiimide (EDCI) and 4,4'-dimethylaminopyridine (DMAP) to furnish **10**, **11** and **12**, respectively (Scheme 3). Coupling of dye **9** with **1**, **2**, or **3** yielded **13**, **14**, and **15**, respectively (Scheme 4). The NMR spectra of all compounds contain the characteristic peaks of the Bodipy and dendron moieties.

Liquid-Crystalline and Thermal Properties. The mesomorphic and thermal properties were investigated by polarized optical microscopy (POM) and differential scanning calorimetry (DSC). All the compounds reported herein show liquid-crystalline properties. The phase-transition temperatures and enthalpies are reported in Table 1. By DSC, melting points were obtained (except for compound **14**) during the first heating run only indicating partial crystalline character of the samples. From the first cooling run, glass transition temperatures were observed for compounds **11** and **12**.

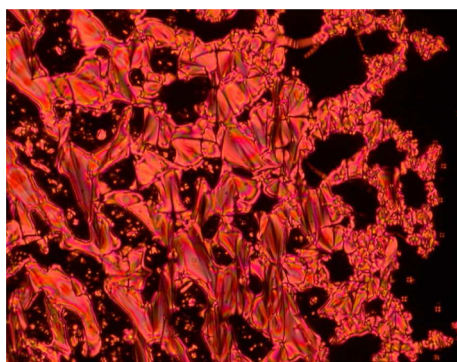
First-Generation Dendrimers. No typical texture was obtained for **13** even when the sample was annealed for several hours near the clearing temperature. Only a birefringent liquid was observed both on heating and cooling the sample. On cooling compound **10** from the isotropic liquid, focal-conic fan

Table 1. Thermal and Liquid-Crystalline Properties with Enthalpy Changes for the Studied Compounds.^a

compd	T_g (°C)	T_m (°C)	ΔH (kJ mol ⁻¹)	transition	T^b (°C)	ΔH (kJ mol ⁻¹)
13		95	35	M → I	129 ^c	13
10		91	53	SmC → SmA SmA → I	105 125	- 13
14				SmA → N N → I	147 149	δ^d
11	55	89	56	SmA → I	156	14
15		102	25	SmA → I	197	28
12	75	102	21	SmA → I	199	28

^a T_g , glass-transition temperature; T_m , melting point (obtained during the first heating run only); M, unidentified mesophase; SmC, smectic C phase; SmA, smectic A phase; N, nematic phase; I, isotropization temperature. ^bTemperatures are given as the onset of the peaks obtained during the second heating run. ^cWith decomposition. ^dCombined enthalpies.

and homeotropic textures were identified that indicated the formation of the smectic A phase (Figure 1). On further cooling,

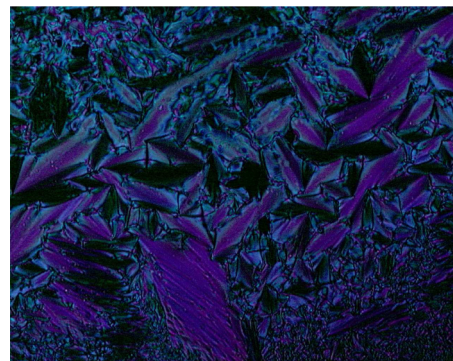
**Figure 1.** Thermal-polarized optical micrograph of the focal-conic fan texture displayed by 10 in the smectic A phase at 124 °C.

modification of the textures was observed by POM at 105 °C indicating a phase transition. No typical texture was obtained for the low-temperature mesophase even after annealing the sample for several hours. As no transition was observed by DSC for this modification, this transition is of second order, and suggests a smectic A-to-smectic C phase transition.

Second-Generation Dendrimers. Nematic (Figure S1 in the Supporting Information, *schlieren* texture) and smectic A phases (Figure 2, focal-conic fan texture) were observed for 14, and a smectic A phase was obtained for 11. An increase in the clearing point on going from the first- to the second-generation dendrimer is observed as a consequence of stronger intermolecular interactions because of a higher number of mesogens when the dendrimer generation increases.

Third-Generation Dendrimers. Compounds 15 and 12 displayed smectic A phases that were identified from the formation of focal-conic fan textures. The latter appeared only when the samples were annealed several hours near the clearing point. Compounds 15 and 12 display the highest clearing points among the materials reported here. The stabilization of mesophases as a function of the number of mesogens is often observed for this kind of dendrimers.³²

The liquid-crystalline phases obtained for compounds 10–15 are in agreement with the structure and nature of the poly(arylester)dendrimers carrying cyanobiphenyl mesogens.

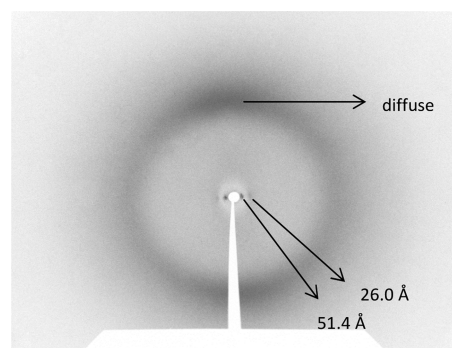
**Figure 2.** Thermal-polarized optical micrograph of the focal-conic fan texture displayed by 14 in the smectic A phase at 139 °C.

Such mesogens have a strong tendency to align parallel one to each other and give rise to the formation of layers as observed for various materials, including liquid-crystalline fullerenes,³³ pillar-[n]arenes ($n = 5$ or 6),³⁴ gold nanoparticles,^{10b} and side-chain polymers.^{35–37} Finally, the liquid-crystalline properties observed for the compounds described herein are in agreement with the properties obtained in our former study based on liquid-crystalline borondipyrromethene dyes.^{9b}

■ X-RAY DIFFRACTION STUDIES

X-ray experiments were carried out on materials submitted to a thermal treatment consisting of heating up the samples into the isotropic liquid and cooling them down slowly into the mesophase or mesomorphic glass (room temperature).

The X-ray patterns of compounds 12, 14, and 15 are consistent with the formation of smectic phases (Figure 3).

**Figure 3.** X-ray pattern of 14 recorded at room temperature after thermal treatment. The sample spontaneously aligned inside the glass capillary by a wall effect on cooling from the isotropic liquid. The capillary axis was horizontal and the image shows that the molecules oriented parallel to the capillary wall yielding a well-aligned pattern.

The patterns contain one or two sharp maxima in the low-angle region and a diffuse halo in the high-angle region. When there are two low-angle maxima, their reciprocal spacing ratio is 1:2, characteristic of a layered structure. The diffuse character of the high-angle halo is typical of disordered SmA and SmC phases. The latter phases are difficult to distinguish on the basis of XRD only, and the determination of the optical textures by POM is a reliable method to assign the actual type of the mesophases.³⁸ For compounds 13, 11, and 10, the X-ray diffractograms do not contain sharp maxima but only diffuse scattering is detected (an illustrative example is shown in Figure S2 in the Supporting Information).

Supramolecular Organization. For compound **14**, the pattern contains two low-angle sharp maxima and a high-angle diffuse halo. Although of relatively weak intensity, low-angle spots are clearly visible and correspond to the first- and second-order reflections from the smectic layers. The measured spacing is 51.4 Å (d_{001}) and 26.0 Å (d_{002}), respectively, and the layer thickness is deduced by the equation $d = (51.4 + 26.0 \times 2)/2 = 51.7$ Å. This value is reasonable for the size of compound **14** packed in a smectic A phase, and is comparable with the smectic layer thickness measured on the smectic A phase of the analogous compound lacking the substituents on the Bodipy ring.^{9b}

For compounds **12** and **15**, the results of the XRD studies are very similar. In both cases, one single low-angle sharp reflection and a high-angle diffuse band are observed in the patterns taken on thermally treated samples. As mentioned above, this kind of pattern is consistent with a smectic phase and is in agreement with the POM observations. For compound **12**, the experimentally measured spacing is 29 Å. This value cannot correspond to the layer thickness because it is too small compared to the length of the molecule. Therefore, the experimentally observed maximum must be the second-order reflection (d_{002}), and thus the layer thickness for compound **12** is 58 Å. For compound **15** ($d_{002} = 26$ Å, layer thickness = 52 Å), the results are qualitatively similar and the conclusions are the same as for compound **12**. The layer thickness values found for these two compounds compare well with the smectic layer thickness measured on the smectic A phase of the analogous compound that has the same structure as **12** and **15** but lacking the substituents on the Bodipy ring.^{9b}

The absence of the first-order reflection for the smectic phase of these two compounds is most likely due to their structures based on alternating sublayers containing the dendritic core (including the Bodipy unit) and the mesogenic units. These two high-generation dendrimers contain eight mesogenic units statistically oriented in both senses with the dendritic core and Bodipy units in the middle. This alternating structure, described for other dendritic systems containing the same mesogenic units,^{8a,9b,39} creates a modulation of the electron density with a period equal to half the full layer thickness. The same phenomenon was reported for liquid-crystalline side-chain polymers,⁴⁰ and was accounted for by the confinement of the polymer backbones in a thin sublayer with the mesogenic units to both sides, so that the backbones (the dendritic core in our case) create an electron density maximum comparable to that of the mesogenic cores.

The absence of X-ray reflections in the diffractograms of **11** and **10** is surprising at first glance, because these compounds show smectic phases as revealed by POM, and this type of mesophases has a long-range interlayer periodicity. However, this phenomenon is not totally unexpected and in fact such a behavior was already observed in our former study.^{9b} The absence of Bragg reflections is accounted for by a poor layering due to a diffuse interface between the smectic layers. The diffuse character of the interface finds its origin in the interdigitation of the cyanobiphenyl units, and this prevents clear diffractograms to be obtained. However, the compounds for which clear diffraction peaks were obtained led to a structural model for the supramolecular organization within the smectic phases (Figure 4).

Spectroscopic Properties and Energy Transfer in the Condensed Phase. The spectroscopic data of the compounds in solution are collected in Table 2. In solution, all compounds show a strong $S_0 \rightarrow S_1$ ($\pi-\pi^*$) transition at 500 nm for the red

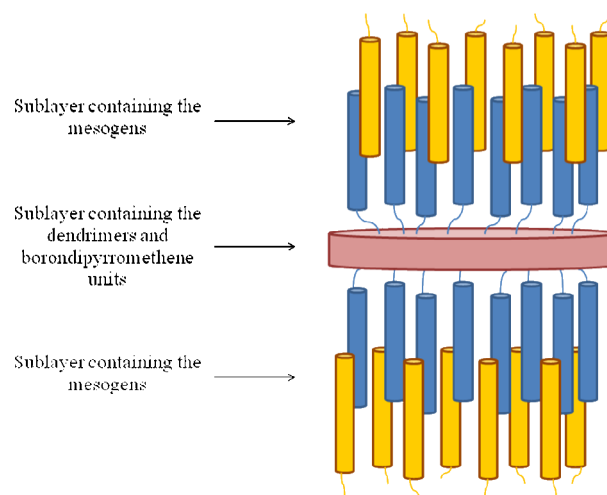


Figure 4. Postulated supramolecular organization of third-generation dendrimers **12** and **15** within the smectic A phase. The interdigitation is illustrated by the yellow and blue cyanobiphenyl units: the blue units belong to the dendrimers which are displayed on the drawing, and the yellow units belong to dendrimers of adjacent layers. Because of the lipophilicity of the Bodipy core, some of the latter groups can also be localized in the sublayers containing the mesogenic units.

family **10**, **11**, and **12**⁴¹ and at 643 nm for the blue family **13**, **14**, and **15**,⁴² characteristic of the Bodipy dyes connected to the dendrimers. In the UV part of the spectra, the contributions of the phenyl groups of the dendrimers are observed with a common hyperchromic shift with increasing the generation of the dendrimers (Figures 5 and 6). The spectral profile is weakly sensitive to solvent polarity (THF, dichloromethane, toluene, dioxane, or DMF) and in keeping with singlet excited states.

Excitation of all compounds in solution in their $S_0 \rightarrow S_1$ transition induces classical emission of the singlet excited state of the central Bodipy dye. The red compounds emit in solution at 511 nm and the blue dyes at 658 nm with a high quantum yields (ca. 60% for the red dyes and about 58% for the blue dyes) and a nanosecond lifetime regime (ca. 4 ns). The low nonradiative rate (k_{NR}), the short lifetime and the shape of the steady-state emission are in good agreement with singlet emitters.⁴³ It is important to mention that the fluorescence was completely quenched in the mesophase: to generate liquid-crystalline phases, heating is required, which most likely favors nonradiative deactivation because of thermal motion enhancement of the molecules.

Solid state emission of pristine compounds **12** and **15** are observed at 576 and 775 nm, respectively (Figures 7 and 8). They are strongly bathochromically shifted and significantly broader versus the same dyes in fluid solution. These spectral shapes are consistent with luminescence of emissive aggregates obtained by stacking the molecules in the solid state (Figures 7 and 8).⁴⁵

When dyes **12** or **15** are diluted in acid **3** (10% weight), a less bathochromically shifted emission is observed. In this solid-solution, the thin and structured emissions observed at 537 and 688 nm, respectively, are likely due to the association of two molecules forming dimers. Such a behavior has previously been observed in thin films of OLED devices engineered from Bodipy dyes.⁴⁶ The dilution of the dye at the solid state induces an enhancement of the fluorescence likely due to the formation of less nonfluorescent aggregates. The solid-state quantum yields measured using an integration sphere at: (i) 0.10 ± 0.02 for **12** as pristine solid at λ_{em} 576 nm and 0.42 ± 0.10 for **12** dispersed at

Table 2. Spectroscopic Data for the Red and Blue Mesomorphic Compounds^a

compd	λ_{abs} (nm)	ϵ ($\times 10^3 \text{ M}^{-1} \text{ cm}^{-1}$)	λ_{em} (nm)	Φ_{F}^b	τ_{s} (ns)	k_{r} ($\times 10^{-8} \text{ s}^{-1}$) ^c	k_{nr} ($\times 10^{-8} \text{ s}^{-1}$) ^c
10	502 278	83.6 173	511	0.60	3.77	1.59	1.06
11	500 277	76.6 230	511	0.61	3.78	1.61	1.03
12	500 278	75.1 409	511	0.67	4.10	1.63	0.81
13	643 269	122 111	658	0.58	4.63	1.25	0.91
14	643 276	102 240	658	0.56	4.28	1.31	1.03
15	644 277	115 392	658	0.60	4.56	1.32	0.87

^aMeasured in THF at 25 °C. ^bDetermined in THF solution, ca. 5×10^{-7} M, using Cresyl Violet as reference ($\phi_{\text{F}} = 0.50$ in ethanol).⁴⁴ All Φ_{F} are corrected for changes in refractive index. ^cCalculated using the following equation: $k_{\text{r}} = \Phi_{\text{F}} / \tau_{\text{F}}$, $k_{\text{nr}} = (1 - \Phi_{\text{F}}) / \tau_{\text{F}}$, assuming that the emitting state is produced with unit quantum efficiency.

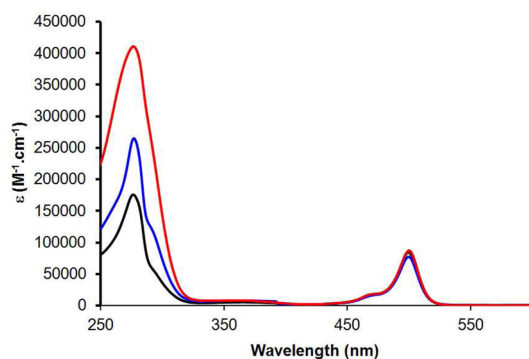


Figure 5. Absorption spectra of compounds 10 (black trace), 11 (blue trace), and 12 (red trace) in THF at room temperature.

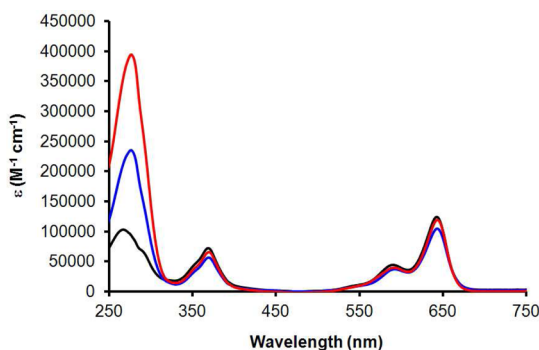


Figure 6. Absorption spectra of compounds 13 (black trace), 14 (blue trace), and 15 (red trace) in THF at room temperature.

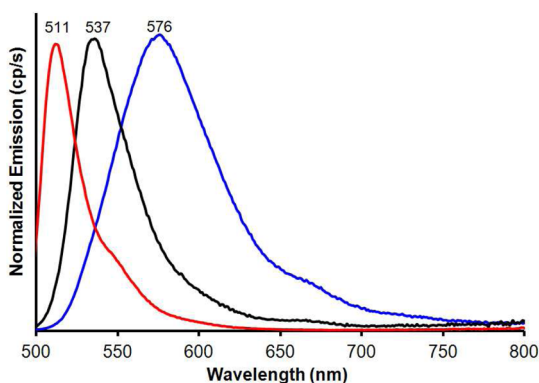


Figure 7. Normalized emission spectra of 12 in 1×10^{-6} M solution in THF (red trace), in the solid state (blue trace) and in 10% solid solution in acid 3 (black trace) at 5×10^{-5} molar.

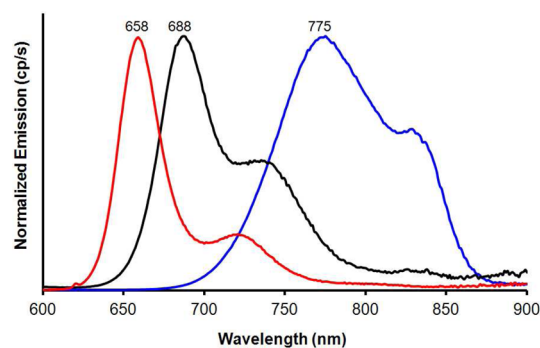


Figure 8. Normalized emission spectra of 15 in 1×10^{-6} M solution in THF (red trace), in the solid state (blue trace), and in 10% solid solution in acid 3 (black trace) at 5×10^{-5} molar.

10% in acid 3 at λ_{em} 537 nm (Figure 7); (ii) <0.01 for 15 as pristine solid at λ_{em} 775 nm and 0.40 ± 0.10 for 15 dispersed at 10% in acid 3 at λ_{em} 688 nm match well the values found in solution (Table 2; 67% for 12 in solution compared to 42% in the solid state, and 60% for 15 in solution compared to 40% in the solid state).

An interesting behavior is observed in the solid-state emission for the 12/15 mixture with decreasing the proportion of dye 15 (energy acceptor) when excited in the absorption band of dye 12 at 480 nm. With a 1:1 to 1:2 ratio of dyes 15/12, no residual emission of donor 12 is detected between 530 and 600 nm, but an intense emission at 736 nm is observed, which is attributed to the 15-aggregates (vide supra). When the ratio of 15 versus 12 is progressively reduced to 1:10, a large emission peak clearly composed of two overlapping emissive bands is observed, leading to the conclusion that different dye arrangements in the solid state are obtained under these conditions (Figure 9). By increasing the dilution process from 1:20 to 1:50, the wavelength shift is less pronounced and the emission profile resembles the one obtained above for the solid-solution of 15 diluted in acid 3 at 10% in weight (Figure 8). Interestingly, when the amount of blue dye is further reduced with respect to the red dye, the energy transfer process is less efficient as observed by the increase in the residual emission of the aggregated dye 12 in the 520 to 620 nm range (Figure 9). For weight proportions of 1 to 1000 (dye 15 to dye 12), dual emission of the aggregated dye 12, aggregated dye 15, and nonaggregated dye 15 appears clearly (green traces in Figure 9).

CONCLUSIONS

Our studies demonstrate that by judicious design of the dendritic platform and Bodipy linker liquid-crystalline materials can be prepared effectively. Because of the nature of the liquid-crystalline promoters, nematic and disordered smectic phases

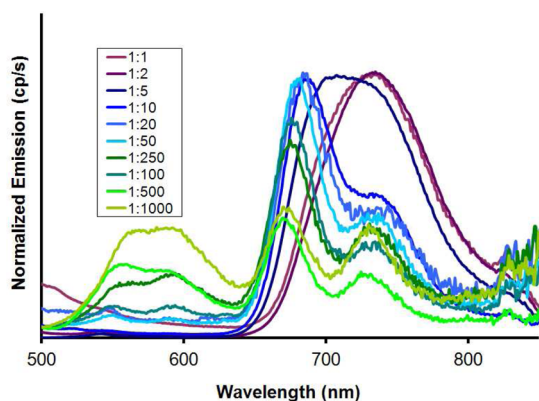


Figure 9. Normalized emission spectra in the solid state of a mixture of **12** (kept constant at 1 molar) and **15** at various ratios, with excitation at 480 nm (filter at 490 nm).

are observed. Interestingly, the pure red and blue materials are fluorescent in the solid state, forming fluorescent aggregates that are bathochromically shifted with respect to the same dyes in solution. Dispersion of the pure materials with the corresponding nonfluorescent acid enhanced the fluorescence quantum yields and shifted the fluorescence to higher energies. High efficiency of energy transfer in the condensed state within films of dyes bearing large dendrimers is clearly evidenced. However, in the liquid-crystalline phases, these materials are completely quenched due to the need of heating of the material. Nonradiative deactivation often appears in a condensed state due to nonradiative deactivation channels favored by motion of the molecules in a hot stage. The role of the dendritic framework to properly disperse the Bodipy dyes in the solid state avoiding formation of nonfluorescent aggregates is evidenced, and quantum yields of about 40% were determined in the solid state under dispersed conditions at ambient temperature.

EXPERIMENTAL SECTION

Synthesis and Characterization of the Compounds. *Compound 4.* A mixture of 2,4-dimethylpyrrole (1.000 g, 10.50 mmol) and *p*-iodobenzoyl chloride (1.370 g, 5.20 mmol) in dry CH_2Cl_2 (50 mL) was stirred at 25 °C for 72 h. The mixture was then treated with Et_3N (0.5 mL), and stirred for another hour. Finally, $\text{BF}_3 \cdot \text{Et}_2\text{O}$ (2.29 mL, 13.8 mmol) was added to the mixture and the solution stirred at 25 °C overnight. The resulting dark mixture was washed with aqueous saturated NaHCO_3 (100 mL), water (50 mL), brine (50 mL) and dried. Removal of solvent in vacuo followed by column chromatography of the residue (flash silica gel, petroleum ether/ethyl acetate) furnished **4** (0.76 g, 32%) as a red powder. IR: 1553, 2880, 2927 cm^{-1} . ^1H NMR: δ 1.40 (s, 6H), 2.72 (s, 6H), 6.01 (s, 2H), 7.05 (d, $J = 8.5$ Hz, 2H), 7.81 (d, $J = 8.5$ Hz, 2H). ^{13}C NMR: δ 14.9, 16.2, 121.8, 129.4, 130.3, 135.2, 138.3, 140.1, 140.9, 155.6. ^{11}B NMR: δ 3.87 (t). EI-MS (m/z , %): 450.06 (M^+ , 100). Anal. Calcd for $\text{C}_{19}\text{H}_{18}\text{BF}_2\text{IN}_2$: C, 50.70; H, 4.03; N, 6.22. Found: C, 50.79; H, 4.17; N, 6.35.

Compound 7. **Compound 4** (304 mg, 0.68 mmol), *p*-methoxybenzaldehyde (92 mg, 0.68 mmol) and piperidine (5 mL) were mixed in toluene (35 mL) and heated under reflux for 3 h. Any water formed during the reaction was removed azeotropically by means of a Dean–Stark trap. Then, the solvent was removed under reduced pressure and the crude product was purified by column chromatography (flash silica gel, petroleum ether/ethyl acetate) to furnish a blue solid **7** (380 mg, 82%). IR: 1598, 2947 cm^{-1} . ^1H NMR: δ 1.48 (s, 6H), 3.86 (s, 6H), 6.62 (s, 2H), 6.92 (d, $J = 8.9$ Hz, 4H), 7.09 (d, $J = 8.3$ Hz, 2H), 7.19 (d, $J = 16.8$ Hz, 2H), 7.55–7.64 (m, 6H), 7.84 (d, $J = 8.3$ Hz, 2H). ^{13}C NMR: δ 14.9, 55.4, 113.6, 114.3, 117.7, 129.1, 129.5, 130.6, 136.1, 138.2, 160.5. ^{11}B NMR: δ 3.87 (t). EI-MS (m/z , %): 686.1 (M^+ , 100); Anal. Calcd for:

$\text{C}_{35}\text{H}_{30}\text{BF}_2\text{IN}_2\text{O}_2$: C, 61.25; H, 4.41; N, 4.08. Found: C, 60.89; H, 4.12; N, 3.72.

Typical Procedure for the Grignard Reaction. To a solution of 4,7-dioxaoct-1-yne (234 mg, 2.05 mmol) in dry THF (30 mL) was added ethylmagnesium bromide (1.71 mL of 1 M THF solution, 1.71 mmol). The mixture was heated at 60 °C during 2 h, cooled to 25 °C, and transferred via canula to a solution of **4/7** (0.68 mmol) in dry THF (20 mL). The mixture was stirred at 25 °C until complete consumption of the starting material was observed by TLC (12 h). Aqueous saturated NH_4Cl (20 mL) was then added into it and the mixture was extracted with CH_2Cl_2 (30 mL). The organic layer was washed with water (20 mL) and brine (20 mL), dried, and evaporated. The residue was purified by column chromatography (flash silica gel, petroleum ether/ethyl acetate) to furnish **5/8**.

Compound 5. Orange powder (303 mg, 70%). IR: 1543, 2882, 2921 cm^{-1} . ^1H NMR: δ 1.40 (s, 6H), 2.72 (s, 6H), 3.36 (s, 6H), 3.52–3.56 (m, 4H), 3.64–3.67 (m, 4H), 4.19 (s, 4H), 6.01 (s, 2H), 7.05 (d, $J = 8.5$ Hz, 2H), 7.81 (d, $J = 8.5$ Hz, 2H). ^{13}C NMR: δ 15.0, 16.2, 59.1, 59.8, 68.7, 71.9, 91.0, 94.6, 121.8, 129.4, 130.4, 135.3, 138.4, 140.1, 141.0, 155.7. ^{11}B NMR: δ –10.00 (s). EI-MS (m/z , %): 638.3 (M^+ , 100). Anal. Calcd For $\text{C}_{31}\text{H}_{36}\text{BIN}_2\text{O}_4$: C, 58.33; H, 5.68; N, 4.39. Found: C, 58.53; H, 5.74; N, 4.19.

Compound 8. Blue powder (383 mg, 65%). IR: 1537, 1599, 2835, 2917 cm^{-1} . ^1H NMR: δ 1.47 (s, 6H), 3.12–3.18 (m, 4H), 3.21 (s, 6H), 3.49–3.55 (m, 4H), 3.87 (s, 6H), 4.18 (s, 4H), 6.64 (s, 2H), 6.91–7.01 (m, 4H), 7.10–7.19 (m, 4H), 7.58 (d, $J = 8.9$ Hz, 4H), 7.84 (d, $J = 8.5$ Hz, 2H), 8.06 (d, $J = 16.3$ Hz, 2H). ^{13}C NMR: δ 15.1, 55.4, 58.7, 59.4, 68.1, 71.5, 91.5, 94.5, 114.3, 114.4, 118.0, 119.0, 128.8, 128.9, 130.0, 130.7, 131.2, 134.0, 134.4, 135.3, 136.7, 138.1, 140.0, 152.1, 153.0, 160.3. ^{11}B NMR: δ –10.00 (s). EI-MS (m/z , %): 874.6 (M^+ , 100). Anal. Calcd For $\text{C}_{47}\text{H}_{48}\text{BIN}_2\text{O}_6$: C, 64.54; H, 5.53; N, 3.20. Found: C, 64.69; H, 5.23; N, 3.35.

Typical Procedure for the Carboamidation Reaction. A stirred solution of **5/8** (0.36 mmol), Et_3N (1.3 mL), ethylenediamine (1.3 mL), and $[\text{Pd}(\text{PPh}_3)_2\text{Cl}_2]$ (48 mg, 0.07 mmol) in toluene (13 mL) was heated at 70 °C under a CO atmosphere until complete consumption of the starting material. H_2O (20 mL) was then added into the mixture and it was extracted with CH_2Cl_2 (50 mL). The organic extract was washed with H_2O (20 mL) and brine (20 mL), dried, and concentrated. The residue was purified by column chromatography (silica gel, $\text{CH}_2\text{Cl}_2/\text{EtOH}$; 80:20) to furnish **6/9**.

Compound 6. Red powder (170 mg, 79%). IR: 1547, 1644, 2871, 2925, 3332 cm^{-1} . ^1H NMR: δ 1.34 (s, 6H), 2.72 (s, 6H), 3.02 (t, $J = 5.6$ Hz, 2H), 3.36 (s, 6H), 3.52–3.61 (m, 6H), 3.63–3.68 (m, 4H), 4.20 (s, 4H), 6.00 (s, 2H), 6.98 (t, $J = 5.6$ Hz, 1H), 7.40 (d, $J = 8.3$ Hz, 2H), 7.94 (d, $J = 8.3$ Hz, 2H). ^{13}C NMR: δ 15.0, 16.2, 41.3, 42.2, 59.1, 59.8, 69.0, 71.9, 90.6, 100.5, 121.9, 127.9, 128.8, 129.4, 134.9, 139.1, 140.4, 141.0, 155.7, 167.0. EI-MS (m/z , %): 598.5 (M^+ , 100). Anal. Calcd For $\text{C}_{34}\text{H}_{43}\text{BN}_4\text{O}_5$: C, 68.23; H, 7.24; N, 9.36; Found: C, 68.42; H, 7.51; N, 9.06. Note amino protons (2H) are not observed, probably because of fast exchange with residual water in the solvent.

Compound 9. Blue powder (177 mg, 59%). IR: 1540, 1598, 2926, 3291 cm^{-1} . ^1H NMR: δ 1.37 (s, 6H), 3.00–3.20 (m, 12H), 3.48–3.60 (m, 6H), 3.85 (s, 6H), 4.16 (s, 4H), 6.60 (s, 2H), 6.93 (d, $J = 8.2$ Hz, 4H), 7.03 (t, $J = 5.8$ Hz, 1H), 7.07 (d, $J = 16.7$ Hz, 2H), 7.40 (d, $J = 7.8$ Hz, 2H), 7.56 (d, $J = 8.2$ Hz, 4H), 7.96–8.14 (m, 4H). ^{13}C NMR: δ 15.2, 38.9, 41.2, 55.5, 58.9, 59.5, 68.3, 71.6, 91.7, 114.6, 118.2, 119.1, 127.9, 129.0, 129.3, 130.1, 131.3, 134.3, 134.8, 137.1, 139.2, 140.1, 152.3, 160.5, 167.2. EI-MS (m/z , %): 834.8 (M^+ , 100). Anal. Calcd For $\text{C}_{50}\text{H}_{55}\text{BN}_4\text{O}_7$: C, 71.94; H, 6.64; N, 6.71. Found: C, 71.99; H, 6.81; N, 6.93. Note amino protons (2H) are not observed, probably because of fast exchange with residual water in the solvent.

Typical Procedure for the Schotten–Baumann Cross-Linking. A mixture of dendron **1/2/3** (0.06 mmol), dye **6/9** (0.07 mmol), EDCI (28 mg, 0.15 mmol), and DMAP (18 mg, 0.15 mmol) in CH_2Cl_2 (70 mL) was stirred at 25 °C until completion of the reaction. The organic layer was thoroughly washed with H_2O (2×10 mL), dried (MgSO_4), and concentrated. The crude product was purified by column chromatography (silica gel, $\text{CH}_2\text{Cl}_2/\text{MeOH}$, 100/0 to 99/1) and crystallized from $\text{CH}_2\text{Cl}_2/\text{CH}_3\text{CN}$ to furnish **10-15**.

Compound 10. Red powder (100 mg, 80%). IR: 1605, 1724, 2228, 2852, 2924, 3322 cm^{-1} . ^1H NMR: δ 1.26–1.53 (m, 42H), 1.71–1.87 (m, 12H), 2.73 (s, 6H), 3.36 (s, 6H), 3.50–3.58 (m, 4H), 3.61–3.70 (m, 4H), 3.76 (s, 4H), 3.80–4.09 (m, 8H), 4.20 (s, 4H), 4.29–4.40 (m, 6H), 6.00 (s, 2H), 6.96 (d, J = 8.7 Hz, 6H), 7.31 (d, J = 8.7 Hz, 4H), 7.40 (d, J = 8.3 Hz, 2H), 7.56–7.76 (m, 12H), 7.88 (d, J = 8.3 Hz, 2H), 7.93 (d, J = 8.3 Hz, 2H), 8.05 (d, J = 1.5 Hz, 2H), 8.14–8.17 (m, 8H), 8.59 (t, J = 1.5 Hz, 1H). ^{13}C NMR: δ 14.8, 16.1, 26.0, 28.7, 29.1, 29.2, 29.3, 29.4, 29.5, 30.9, 41.2, 41.3, 58.9, 59.7, 65.5, 65.8, 68.4, 68.6, 71.8, 90.9, 111.0, 114.4, 114.5, 118.9, 120.8, 121.2, 121.8, 122.6, 127.2, 127.3, 127.7, 127.9, 128.3, 128.8, 129.2, 129.8, 132.3, 132.4, 132.7, 133.2, 134.3, 136.7, 137.8, 139.1, 140.3, 140.8, 144.9, 151.2, 151.7, 155.6, 163.8, 163.9, 164.6, 164.9, 165.1, 165.9, 167.8, 167.9. MALDI-TOF (m/z , %): 2114.4 (M^+ , 100). Anal. Calcd for $\text{C}_{127}\text{H}_{137}\text{BN}_8\text{O}_{21}\cdot\text{H}_2\text{O}$: C, 72.21; H, 6.63; N, 3.98. Found: C, 72.32; H, 6.98; N, 4.12.

Compound 11. Red powder (156 mg, 78%). IR: 1604, 1727, 2227, 2854, 2924, 3322 cm^{-1} . ^1H NMR: δ 1.24–1.47 (m, 66H), 1.77–1.85 (m, 20H), 2.73 (s, 6H), 3.35 (s, 6H), 3.50–3.56 (m, 4H), 3.62–3.69 (m, 4H), 3.73 (s, 4H), 3.98–4.06 (m, 12H), 4.19 (s, 4H), 4.29–4.40 (m, 12H), 5.99 (s, 2H), 6.95 (d, J = 8.7 Hz, 10H), 7.29 (d, J = 8.3 Hz, 8H), 7.36 (d, J = 7.9 Hz, 2H), 7.57–7.74 (m, 24H), 7.88 (d, J = 8.3 Hz, 2H), 7.94 (d, J = 8.3 Hz, 2H), 8.04–8.19 (m, 14H), 8.35 (d, J = 1.5 Hz, 2H), 8.63 (t, J = 1.5 Hz, 2H), 8.93 (t, J = 1.5 Hz, 1H). ^{13}C NMR: δ 14.8, 16.2, 26.0, 26.1, 28.7, 29.2, 29.3, 29.4, 29.5, 29.6, 31.0, 41.2, 41.4, 59.0, 59.7, 65.6, 65.9, 68.4, 68.7, 71.8, 91.0, 111.1, 114.5, 114.7, 118.9, 120.4, 121.3, 121.8, 122.6, 127.1, 127.2, 127.7, 127.9, 128.4, 128.5, 128.8, 129.1, 129.2, 129.9, 133.2, 134.2, 136.7, 137.8, 139.2, 140.2, 140.8, 144.9, 150.7, 151.7, 151.8, 155.7, 163.1, 163.8, 164.2, 164.5, 164.8, 164.9, 165.9, 167.9, 168.1. MALDI-TOF (m/z , %): 3370.0 (M^+ , 100). Anal. Calcd for $\text{C}_{203}\text{H}_{207}\text{BN}_8\text{O}_{35}\cdot\text{H}_2\text{O}$: C, 73.83; H, 6.29; N, 3.35. Found: C, 72.54; H, 6.61; N, 3.40.

Compound 12. Red powder (185 mg, 53%). IR: 1606, 1725, 2230, 2850, 2936, 3331 cm^{-1} . ^1H NMR: δ 1.32 (m, 80H), 1.78 (m, 40H), 2.73 (s, 6H), 3.36 (s, 6H), 3.54 (m, 4H), 3.66 (m, 4H), 3.74 (s, 4H), 4.03 (m, 22H), 4.20 (s, 6H), 4.37 (m, 20H), 6.00 (s, 2H), 6.96 (d, J = 8.9 Hz, 18H), 6.98 (d, J = 8.1 Hz, 3H), 7.28 (d, J = 8.6 Hz, 18H), 7.38 (d, J = 8.1 Hz, 3H), 7.61 (d, J = 8.6 Hz, 20H), 7.70 (ABq, J = 7.6 Hz, 38H), 7.92 (d, J = 8.1 Hz, 6H), 8.13 (m, 33H), 8.41 (s, 6H), 8.64 (s, 5H), 8.98 (s, 3H). ^{13}C NMR: δ 14.8, 16.1, 25.9, 26.0, 28.7, 29.2, 29.3, 29.4, 29.5, 29.6, 59.0, 59.7, 65.9, 68.4, 68.6, 71.8, 111.0, 114.4, 114.6, 118.9, 121.2, 121.8, 122.6, 127.0, 127.2, 127.7, 127.8, 128.4, 128.5, 128.8, 129.2, 129.8, 131.4, 132.4, 132.7, 136.7, 140.8, 140.8, 150.5, 150.6, 155.6, 162.9, 163.7, 164.2, 164.4, 164.8, 164.9, 165.9, 167.8, 168.1. MALDI-TOF (m/z , %): 5816.2 (M^+ , 100). Anal. Calcd for $\text{C}_{355}\text{H}_{347}\text{BN}_{12}\text{O}_{63}\cdot\text{H}_2\text{O}$: C, 73.28; H, 6.05; N, 2.89. Found: C, 73.69; H, 6.51; N, 3.15.

Compound 13. Blue powder (71 mg, 51%). IR: 1601, 1722, 2226, 2854, 2925, 3301 cm^{-1} . ^1H NMR: δ 1.28–1.49 (m, 42H), 1.72–1.84 (m, 12H), 3.13–3.20 (m, 12H), 3.49–3.55 (m, 4H), 3.72 (s, 4H), 3.85 (s, 6H), 3.99–4.08 (m, 6H), 4.16 (s, 4H), 4.29–4.39 (m, 6H), 6.59 (s, 2H), 6.93–7.00 (m, 10H), 7.10 (d, J = 16.2 Hz, 2H), 7.30 (d, J = 8.3 Hz, 4H), 7.40 (d, J = 7.9 Hz, 2H), 7.56–7.75 (m, 16H), 7.89 (d, J = 8.3 Hz, 2H), 7.94 (d, J = 8.3 Hz, 2H), 8.03–8.17 (m, 12H), 8.59 (t, J = 1.5 Hz, 1H). ^{13}C NMR: δ 15.1, 26.1, 28.8, 29.2, 29.3, 29.4, 29.5, 29.6, 41.3, 41.5, 55.5, 58.9, 59.5, 65.6, 65.9, 68.4, 68.5, 71.6, 91.7, 111.1, 114.5, 114.6, 118.2, 119.0, 119.1, 120.9, 121.4, 122.7, 127.2, 127.4, 127.8, 128.0, 128.4, 129.0, 129.4, 129.9, 130.1, 131.2, 132.4, 132.5, 132.6, 132.8, 133.4, 134.3, 136.8, 137.0, 137.8, 139.5, 140.0, 151.2, 151.7, 152.3, 160.5, 163.8, 164.0, 164.7, 164.9, 165.2, 166.0, 167.9. MALDI-TOF (m/z , %): 2350.7 (M^+ , 100). Anal. Calcd for $\text{C}_{143}\text{H}_{149}\text{BN}_6\text{O}_{23}\cdot\text{H}_2\text{O}$: C, 73.13; H, 6.48; N, 3.58. Found: C, 73.29; H, 6.41; N, 3.65.

Compound 14. Blue powder (108 mg, 50%). IR: 1604, 1727, 2227, 2854, 2924, 3322 cm^{-1} . ^1H NMR: δ 1.24–1.51 (m, 66H), 1.72–1.86 (m, 24H), 3.14–3.20 (m, 10H), 3.50–3.54 (m, 4H), 3.75 (s, 4H), 3.85 (s, 6H), 3.98–4.06 (m, 10H), 4.16 (s, 4H), 4.28–4.40 (m, 10H), 6.60 (s, 2H), 6.93–7.01 (m, 12H), 7.10 (d, J = 16.2 Hz, 2H), 7.29 (d, J = 8.5 Hz, 8H), 7.40 (d, J = 8.1 Hz, 2H), 7.56–7.74 (m, 30H), 7.89 (d, J = 8.5 Hz, 2H), 7.95 (d, J = 8.1 Hz, 2H), 8.05–8.23 (m, 16H), 8.35 (d, J = 1.3 Hz, 2H), 8.63 (t, J = 1.3 Hz, 2H), 8.93 (t, J = 1.3 Hz, 1H). ^{13}C NMR: δ 15.1, 26.0, 26.1, 28.8, 29.2, 29.3, 29.4, 29.5, 29.6, 31.0, 41.2, 41.5, 55.5, 58.9, 59.5, 65.6, 66.0, 68.3, 68.4, 68.5, 68.6, 71.6, 91.0, 111.0, 111.1,

114.5, 114.6, 114.7, 118.2, 119.0, 119.1, 120.4, 120.8, 121.4, 122.7, 127.1, 127.2, 127.8, 128.4, 128.5, 129.0, 129.2, 129.4, 129.9, 130.1, 131.2, 131.3, 132.3, 132.4, 132.7, 132.8, 133.4, 134.2, 134.3, 136.8, 137.8, 140.0, 145.0, 150.7, 151.7, 152.4, 160.5, 163.2, 163.8, 164.2, 164.6, 164.9, 165.0, 165.9, 168.0, 168.3. MALDI-TOF (m/z , %): 3606.2 (M^+ , 100). Anal. Calcd for $\text{C}_{219}\text{H}_{219}\text{BN}_8\text{O}_{37}\cdot\text{H}_2\text{O}$: C, 73.39; H, 6.22; N, 3.13. Found: C, 73.09; H, 6.45; N, 3.25.

Compound 15. Blue powder (148 mg, 41%). IR: 1602, 1725, 2232, 2858, 2929, 3330 cm^{-1} . ^1H NMR: δ 1.34 (m, 52H), 1.46 (m, 32H), 1.79 (m, 24H), 3.20 (s, 6H), 3.52 (m, 14H), 3.86 (s, 6H), 4.03 (m, 26H), 4.17 (s, 6H), 4.35 (m, 32H), 6.61 (s, 2H), 6.96 (d, J = 8.9 Hz, 24H), 7.12 (d, J = 16.1 Hz, 2H), 7.31 (d, J = 8.1 Hz, 24H), 7.45 (d, J = 8.1 Hz, 3H), 7.62 (d, J = 8.6 Hz, 22H), 7.70 (ABq, J = 7.6 Hz, 32H), 7.91 (d, J = 8.1 Hz, 6H), 8.12 (m, 32H), 8.40 (s, 6H), 8.63 (s, 5H), 8.98 (s, 3H). ^{13}C NMR: δ 14.9, 25.9, 26.0, 28.7, 29.1, 29.3, 29.4, 29.5, 29.5, 55.4, 58.8, 59.5, 65.5, 65.9, 68.2, 68.4, 71.6, 111.0, 114.4, 114.5, 114.6, 118.0, 118.9, 119.0, 121.2, 122.6, 127.0, 127.1, 127.7, 128.4, 128.5, 128.8, 129.3, 129.6, 129.9, 130.0, 130.9, 131.1, 132.4, 132.4, 132.7, 134.2, 136.7, 139.9, 144.9, 150.5, 151.0, 151.6, 152.2, 160.4, 162.9, 163.0, 163.7, 164.8, 164.9, 165.9, 167.8, 168.1. Anal. Calcd for $\text{C}_{371}\text{H}_{359}\text{BN}_{12}\text{O}_{65}\cdot\text{H}_2\text{O}$: C, 73.60; H, 6.01; N, 2.78. Found: C, 73.53; H, 5.25; N, 2.54.

■ ASSOCIATED CONTENT

Supporting Information

Techniques, instruments, and analytical data of the new compounds. This material is available free of charge via the Internet at <http://pubs.acs.org/>.

■ AUTHOR INFORMATION

Corresponding Authors

*E-mail: ziessel@unistra.fr.

*E-mail: jbarbera@unizar.es.

*E-mail: robert.deschenaux@unine.ch.

Present Address

*S.M. is currently at Bio-Organic Division, Bhabha Atomic Research Centre, Mumbai 400085, India

Notes

The authors declare no competing financial interest.

■ ACKNOWLEDGMENTS

R.D. thanks the Swiss National Science Foundation (Grants 200020-140298 and 200020-152716) for financial support. J.B. thanks the MINECO, Spain, for financial support under the project CTQ2012-35692, which included FEDER funding. We acknowledge the CNRS and the Ministère de l'Enseignement Supérieur de la Recherche for providing research facilities and some financial support. S.M. is very grateful to the French Embassy in India for the award of a Sandwich-PhD scholarship and to the Bhabha Atomic Research Center for permission to conduct research in France. We also thank Delphine Hablot and Dr. Jean-Hubert Olivier for providing Bodipy Starting materials.

■ REFERENCES

- (1) (a) Hosomizu, K.; Imahori, H.; Hahn, U.; Nierengarten, J.-F.; Listorti, A.; Armaroli, N.; Nemoto, T.; Isoda, S. *J. Phys. Chem. C* **2007**, *111*, 2777–2786. (b) Lin, B. F.; Marullo, R. S.; Robb, M. J.; Krogstad, D. V.; Antoni, P.; Hawker, C. J.; Campos, L. M.; Tirrell, M. V. *Nano Lett.* **2011**, *11*, 3946–3950. (c) Tomalia, D. A. *New J. Chem.* **2012**, *36*, 264–281. (d) Mignani, S.; Majoral, J.-P. *New J. Chem.* **2013**, *37*, 3337–3357.
- (2) Tekade, R. K.; Kumar, P. V.; Jain, N. K. *Chem. Rev.* **2009**, *109*, 49–87.
- (3) Percec, V.; Leowanawat, P.; Sun, H.-J.; Kulikov, O.; Nusbaum, C. D.; Tran, T. M.; Bertin, A.; Wilson, D. A.; Peterca, M.; Zhang, S.; Karnat, N. P.; Vargo, K.; Moock, D.; Johnston, E. D.; Hammer, D. A.; Pochan, D. J.; Chen, Y.; Chabre, Y. M.; Shiao, T. C.; Bergeron-Brek, M.; André, S.;

Roy, R.; Gabius, H.-J.; Heiney, P. A. *J. Am. Chem. Soc.* **2013**, *135*, 9055–9077 and references cited therein.

(4) Roche, C.; Percec, V. *Isr. J. Chem.* **2013**, *53*, 30–44.

(5) Selected publications on fullerene-containing liquid crystals:

(a) Lincker, F.; Bourgun, P.; Stoekli-Evans, H.; Saez, I. M.; Goodby, J. W.; Deschenaux, R. *Chem. Commun.* **2010**, *46*, 7522–7524.

(b) Campidelli, S.; Bourgun, P.; Guintchin, B.; Furrer, J.; Stoekli-Evans, H.; Saez, I. M.; Goodby, J. W.; Deschenaux, R. *J. Am. Chem. Soc.* **2010**, *132*, 3574–3581.

(c) Hoang, T. N. Y.; Pocięcha, D.; Salamonczyk, M.; Gorecka, E.; Deschenaux, R. *Soft Matter* **2011**, *7*, 4948–4953.

(d) Li, H.; Hollamby, M. J.; Seki, T.; Yagai, S.; Mōhwald, H.; Nakanishi, T. *Langmuir* **2011**, *27*, 7493–7501.

(e) Vergara, J.; Barberá, J.; Serrano, J. L.; Ros, M. B.; Sebastián, N.; de la Fuente, R.; López, D. O.; Fernández, G.; Sánchez, L.; Martín, N. *Angew. Chem., Int. Ed.* **2011**, *50*, 12523–12528.

(f) Ince, M.; Martínez-Díaz, M. V.; Barberá, J.; Torres, T. *J. Mater. Chem.* **2011**, *21*, 1531–1536.

(g) Mamlouk-Chaouachi, H.; Heinrich, B.; Bourgogne, C.; Guillon, D.; Donnio, B.; Felder-Flesch, D. *J. Mater. Chem.* **2011**, *21*, 9121–9129.

(h) Zhang, X.; Hsu, C.-H.; Ren, X.; Gu, Y.; Song, B.; Sun, H.-J.; Yang, S.; Chen, E.; Tu, Y.; Li, X.; Yang, X.; Li, Y.; Zhu, X. *Angew. Chem., Int. Ed.* **2015**, *54*, 114–117.

(i) Lehmann, M.; Hügel, M.; *Angew. Chem., Int. Ed.* **2015**, *54*, DOI: 10.1002/anie.201410662.

(6) Review on ferrocene-containing liquid crystals: Kadkin, O. N.; Galyametdinov, Y. G. *Russ. Chem. Rev.* **2012**, *81*, 675–699.

(7) Campidelli, S.; Severac, M.; Scanu, D.; Deschenaux, R.; Vázquez, E.; Milic, D.; Prato, M.; Carano, M.; Marcaccio, M.; Paolucci, F.; Rahman, G. M. A.; Guldí, D. M. *J. Mater. Chem.* **2008**, *18*, 1504–1509.

(8) (a) Frein, S.; Auzias, M.; Sondenecker, A.; Vieille-Petit, L.; Guintchin, B.; Maringa, N.; Süß-Fink, G.; Barberá, J.; Deschenaux, R. *Chem. Mater.* **2008**, *20*, 1340–1343.

(b) Chaia, Z. D.; Rusjan, M. C.; Castro, M. A.; Donnio, B.; Heinrich, B.; Guillon, D.; Baggio, R. F.; Cukiernik, F. D. *J. Mater. Chem.* **2009**, *19*, 4981–4991.

(c) Bottazzi, T.; Cecchi, F.; Zelcer, A.; Heinrich, B.; Donnio, B.; Guillon, D.; Cukiernik, F. D. *J. Coord. Chem.* **2013**, *66*, 3380–3390.

(9) (a) Chen, Z.; Swager, T. M. *Org. Lett.* **2007**, *9*, 997–1000.

(b) Frein, S.; Camerel, F.; Ziessel, R.; Barberá, J.; Deschenaux, R. *Chem. Mater.* **2009**, *21*, 3950–3959.

(c) Kendhale, A. M.; Schenning, A. P. H. J.; Debije, M. G. *J. Mater. Chem. A* **2013**, *1*, 229–232.

(10) (a) Donnio, B.; García-Vázquez, P.; Gallani, J.-L.; Guillon, D.; Terrazi, E. *Adv. Matter.* **2007**, *19*, 3534–3539.

(b) Mischler, S.; Guerra, S.; Deschenaux, R. *Chem. Commun.* **2012**, *48*, 2183–2185.

(c) Yu, C. H.; Schubert, C. P. J.; Welch, C.; Tang, B. J.; Tamba, M.-G.; Mehl, G. H. *J. Am. Chem. Soc.* **2012**, *134*, 5076–5079.

(d) Kanie, K.; Matsubara, M.; Zeng, X.; Liu, F.; Ungar, G.; Nakamura, H.; Muramatsu, A. *J. Am. Chem. Soc.* **2012**, *134*, 808–811.

(e) Lewandowski, W.; Jatczak, K.; Pocięcha, D.; Mieczkowski, J. *Langmuir* **2013**, *29*, 3404–3410.

(f) Lewandowski, W.; Constantin, D.; Walicka, K.; Pocięcha, D.; Mieczkowski, J.; Górecka, E. *Chem. Commun.* **2013**, *49*, 7845–7847.

(g) Romiszewski, J.; Puterová-Tokarová, Z.; Mieczkowski, J.; Gorecka, E. *New J. Chem.* **2014**, *38*, 2927–2934.

(h) Wolska, J. M.; Pocięcha, D.; Mieczkowski, J.; Górecka, E. *Chem. Commun.* **2014**, *50*, 7975–7978.

(11) Sagara, Y.; Kato, T. *Angew. Chem., Int. Ed.* **2008**, *47*, 5175–5178.

(12) Wang, Y.; Chen, Q.; Li, Y.; Liu, Y.; Tan, H.; Yu, J.; Zhu, M.; Wu, H.; Zhu, W.; Cao, Y. *J. Phys. Chem. C* **2012**, *116*, 5908–5914.

(13) (a) Venkatesan, K.; Kouwer, P. H. J.; Yagi, S.; Müller, P.; Swager, T. M. *J. Mater. Chem.* **2008**, *18*, 400–407.

(b) Thomas, S. W.; Yagi, S.; Swager, T. M. *J. Mater. Chem.* **2005**, *15*, 2829–2835.

(c) Damm, C.; Israel, G.; Hegmann, T.; Tschierske, C. *J. Mater. Chem.* **2006**, *16*, 1808–1816.

(d) Santoro, A.; Whitwood, A. C.; Williams, J. A. G.; Kozhevnikov, V. N.; Bruce, D. W. *Chem. Mater.* **2009**, *21*, 3871–3882.

(14) (a) Hu, J.; Zhang, D.; Jin, S.; Cheng, S. Z. D.; Harris, F. W. *Chem. Mater.* **2004**, *16*, 4912–4915.

(b) Leng, S.; Chan, L. H.; Jing, J.; Hu, J.; Moustafa, R. M.; Van Horn, R. M.; Graham, M. J.; Sun, B.; Zhu, M.; Jeong, K. U.; Kaafarani, B. R.; Zhang, W.; Harris, F. W.; Cheng, S. Z. D. *Soft Matter* **2010**, *6*, 100–112.

(c) Gao, B.; Wang, M.; Cheng, Y.; Wang, L.; Jing, X.; Wang, F. *J. Am. Chem. Soc.* **2008**, *130*, 8297–8306.

(d) Lucas, L. A.; De Longchamp, D. M.; Richter, L. J.; Kline, R. J.; Fischer, D. A.; Kaafarani, B. R.; Jabbour, G. E. *Chem. Mater.* **2008**, *20*, 5743–5749.

(e) Leng, S.; Wex, B.; Chan, L. H.; Graham, M. J.; Jin, S.;

Jing, A. J.; Jeong, K. U.; Van Horn, R. M.; Sun, B.; Zhu, M.; Kaafarani, B. R.; Cheng, S. Z. D. *J. Phys. Chem. B* **2009**, *113*, 5403–5411.

(f) Chen, S.; Raad, F. S.; Ahmida, M.; Kaafarani, B. R.; Eichhorn, S. H. *Org. Lett.* **2013**, *15*, 558–561.

(g) Chen, C.-C.; Hinoue, T.; Hisaki, I.; Miyata, M.; Tohnai, N. *Tetrahedron Lett.* **2013**, *54*, 1649–1653.

(15) (a) Jin, H.; Zheng, Y.; Liu, Y.; Cheng, H.; Zhou, Y.; Yan, D. *Angew. Chem., Int. Ed.* **2011**, *50*, 10352–10356.

(b) Nalluri, S. K. M.; Voskuhl, J.; Bultema, J. B.; Boekema, E. J.; Ravoo, B. J. *Angew. Chem., Int. Ed.* **2011**, *50*, 9747–9751.

(16) Kozhevnikov, V. N.; Donnio, B.; Bruce, D. W. *Angew. Chem., Int. Ed.* **2008**, *47*, 6286–6289.

(17) Liu, Y.; Yu, C.; Jin, H.; Jiang, B.; Zhu, X.; Zhou, Y.; Lu, Z.; Yan, D. *J. Am. Chem. Soc.* **2013**, *135*, 4765–4770.

(18) (a) Santoro, A.; Whitwood, A. C.; Williams, J. A. G.; Kozhevnikov, V. N.; Bruce, D. W. *Chem. Mater.* **2009**, *21*, 3871–3882.

(b) Spencer, M.; Santoro, A.; Freeman, G. R.; Díez, Á.; Murray, P. R.; Torroba, J.; Whitwood, A. C.; Yellowlees, L. J.; Williams, J. A. G.; Bruce, D. W. *Dalton Trans.* **2012**, *41*, 14244–14256.

(19) Prokhorov, A. M.; Santoro, A.; Williams, J. A. G.; Bruce, D. W. *Angew. Chem., Int. Ed.* **2012**, *51*, 95–98.

(20) Micutz, M.; Iliš, M.; Staicu, T.; Dumitrascu, F.; Pasuk, I.; Molard, Y.; Roisnel, T.; Circu. *Dalton Trans.* **2014**, *43*, 1151–1161.

(21) Iliš, M.; Micutz, M.; Dumitrascu, F.; Pasuk, I.; Molard, Y.; Roisnel, T.; Circu, V. *Polyhedron* **2014**, *69*, 31–39.

(22) Cortes, M. A.; Dorson, F.; Prévôt, M.; Ghoufi, A.; Fontaine, B.; Goujon, F.; Gautier, R.; Circu, V.; Mériadec, C.; Artzner, F.; Follot, H.; Cordier, S.; Molard, Y. *Chem.—Eur. J.* **2014**, *20*, 8561–8565.

(23) Camerel, F.; Bonardi, L.; Schmutz, M.; Ziessel, R. *J. Am. Chem. Soc.* **2006**, *128*, 4548–4549.

(24) Camerel, F.; Bonardi, L.; Ulrich, G.; Charbonnière, L.; Donnio, B.; Bourgogne, C.; Guillon, D.; Retailleau, P.; Ziessel, R. *Chem. Mater.* **2006**, *18*, 5009–5021.

(25) Olivier, J.-H.; Barberá, J.; Bahaidarah, E.; Harriman, A.; Ziessel, R. *J. Am. Chem. Soc.* **2012**, *134*, 6100–6103.

(26) Ziessel, R.; Bonardi, L.; Retailleau, P.; Ulrich, G. *J. Org. Chem.* **2006**, *71*, 3093–3102.

(27) Mula, S.; Elliot, K.; Harriman, A.; Ziessel, R. *J. Phys. Chem. A* **2010**, *114*, 10515–10522.

(28) Kolmakov, K.; Belov, V. N.; Wurm, C. A.; Harke, B.; Leutenegger, M.; Eggeling, C.; Hell, S. W. *Eur. J. Org. Chem.* **2010**, 3593–3610.

(29) Rousseau, T.; Cravino, A.; Bura, T.; Ulrich, G.; Ziessel, R.; Roncali, J. *Chem. Commun.* **2009**, 1673–1675.

(30) Ziessel, R.; Bura, T.; Olivier, J.-H. *Synlett.* **2010**, 2304–2310.

(31) El-ghayoury, A.; Ziessel, R. *J. Org. Chem.* **2000**, *65*, 7757–7763.

(32) Dardel, B.; Guillon, D.; Heinrich, B.; Deschenaux, R. *J. Mater. Chem.* **2001**, *11*, 2814–2831.

(33) Lenoble, J.; Campidelli, S.; Maringa, N.; Donnio, B.; Guillon, D.; Yevlampieva, N.; Deschenaux, R. *J. Am. Chem. Soc.* **2007**, *129*, 9941–9952.

(34) (a) Nierengarten, I.; Guerra, S.; Holler, M.; Nierengarten, J.-F.; Deschenaux, R. *Chem. Commun.* **2012**, *48*, 8072–8074.

(b) Nierengarten, I.; Guerra, S.; Holler, M.; Karmazin-Brelot, L.; Barberá, J.; Deschenaux, R.; Nierengarten, J.-F. *Eur. J. Org. Chem.* **2013**, 3675–3684.

(35) Kawakami, T.; Kato, T. *Macromolecules* **1998**, *31*, 4475–4479.

(36) Yamada, M.; Itoh, T.; Nakagawa, R.; Hirao, A.; Nakahama, S.-i.; Watanabe, J. *Macromolecules* **1999**, *32*, 282–289.

(37) Barmatov, E. B.; Filippov, A. P.; Shibaev, V. P. *Liq. Cryst.* **2001**, *28*, 511–523.

(38) (a) Cowling, S. J. Optical Microscopy Studies of Liquid Crystals. In *Handbook of Liquid Crystals*; Goodby, J. W., Collings, P. J., Kato, T., Tschierske, C., Gleeson, H. F., Raynes, P., Eds.; Wiley-VCH: Weinheim, Germany, 2014; Vol. 1, Chapter 9.

(b) Agra-Kooijman, D. M., Kumar, S. X-ray Investigations of Liquid Crystals. In *Handbook of Liquid Crystals*; Goodby, J. W., Collings, P. J., Kato, T., Tschierske, C., Gleeson, H. F., Raynes, P., Eds.; Wiley-VCH: Weinheim, Germany, 2014; Vol. 1, Chapter 10.

(39) Campidelli, S.; Lenoble, J.; Barberá, J.; Paolucci, F.; Marcaccio, M.; Paolucci, D.; Deschenaux, R. *Macromolecules* **2005**, *38*, 7915–7925.

- (40) (a) Davidson, P.; Levelut, A. M.; Achard, M. F.; Hardouin, F. *Liq. Cryst.* **1989**, *4*, 561–571. (b) Barberá, J.; Giorgini, L.; Paris, F.; Salatelli, E.; Tejedor, R. M.; Angiloini, L. *Chem.—Eur. J.* **2008**, *14*, 11209–11221.
- (41) Ziessel, R.; Ulrich, G.; Harriman, A. *New J. Chem.* **2007**, *31*, 496–501.
- (42) Ulrich, G.; Ziessel, R.; Harriman, A. *Angew. Chem., Int. Ed.* **2008**, *47*, 1184–1201.
- (43) Karolin, J.; Johansson, L. B.-A.; Strandberg, L.; Ny, T. *J. Am. Chem. Soc.* **1994**, *116*, 7801–7806.
- (44) Olmsted, J., III *J. Phys. Chem.* **1979**, *83*, 2581–2584.
- (45) Olivier, J.-H.; Widmaier, J.; Ziessel, R. *Chem.—Eur. J.* **2011**, *17*, 11709–11714.
- (46) Bonardi, L.; Kanaan, H.; Camerel, F.; Jolinat, P.; Retailleau, P.; Ziessel, R. *Adv. Funct. Mater.* **2008**, *18*, 401–413.